Dyes and Pigments 239 (2025) 112785

Contents lists available at ScienceDirect

Dyes and Pigments

journal homepage: www.elsevier.com/locate/dyepig

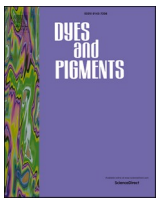

Design and synthesis of quadrupolar A-D-A photon absorbing molecules: An investigation into their optical and bioimaging properties

Shufan Yang [a,b], Konstantinos Bourdakos [c], Hiroki Cook [c], Anna Crisford [c], Ewan Forsyth [a], Sumeet Mahajan [c], Mark Bradley [b,*]

[a] School of Chemistry, University of Edinburgh, David Brewster Road, EH9 3FJ, United Kingdom
[b] Precision Healthcare University Research Institute, Queen Mary University of London, Empire House, 67 New Road, E1 1HH, United Kingdom
[c] University of Southampton, School of Chemistry, Faculty of Engineering and Physical Sciences, Southampton, United Kingdom

A B S T R A C T

We herein report on the design and synthesis and optical properties of 4 novel chromophores based on a quadrupole acceptor-donor-acceptor system. These quadrupoles were designed using a fluorene core, coupled to thienyl and thienyl acetylene bridges, to either two 3-dicycanovinylindan-1-ones or two 1,3-bis(dicyanomethylidene)-indanes as strong electron-withdrawing moieties. The structure-property relationships were investigated by computational modelling and photophysical studies, with the fluorophores giving red-emission with large Stokes shifts. The bridged alkynyl units, rather than enhancing conjugation, dramatically reduced fluorescence intensities and wavelength of emission. Notably, two-photon absorption studies revealed cross-section values of $\delta = 1720$ and 780 GM for two of the fluorophores. The fluorophores were explored in one-photon and two-photon fluorescence biological imaging, including the staining of chick bones.

1. Introduction

In the realm of generating new fluorophores, fused-ring dyes based on an Acceptor-Donor-Acceptor (A-D-A) scaffold comprise an electron-rich donor core flanked on either side by electron-deficient acceptor groups [1–7]. They offer access to a huge number of structural options, although the choice of donor and acceptor groups in the absorbing fused-ring systems is critical. Importantly, the centrosymmetrical nature of A-D-A dyes has important implications on their photo-physical properties. It can cause symmetry breaking in the excited state, resulting in a strong sensitivity to polarity [8,9] and significant Stokes shifts [10]. In addition, the choice of the A-D-A building blocks can provide two-photon (2P) excitation properties [11] (the ability to "simultaneously'' absorb two photons and emit one photon of higher energy [12]) and determines the electronic and steric interactions that ultimately govern the dye's optical efficiency and stability [11].

Most of the current literature [13–17] is based on compounds that absorb two photons in the wavelength regions of the visible (520–700 nm) and near-infrared (700–900 nm) [13] spectrum. In recent years, molecules that absorb in thealled NIR-II (900–1700 nm) or short-IR biological window (770–1400 nm) [18–20] have being explored as this allows greater depth of penetration, predominately due to reduced scattering [21]. This makes them extremely useful in fields, such as bioimaging, while such molecules would also be beneficial in the area of photodynamic therapy, where two photon excitation would allow deeper, more localised, singlet oxygen generation for the treatment of tumours or deep seated bacterial infections [22–24]. Structurally, such dyes tend to have extended conjugation, crucial for their capability to absorb lower-energy photons [25–27]. These properties can be chemically tuned and this flexibility allows for the creation of dyes that can be tailored for specific imaging applications, with control of their brightness and excitation cross-sectional areas always a key consideration [28–31]. In addition, stability is a key factor for any two-photon absorption (2PA) dye, with the need to resist photobleaching, vital for the high powers and extended imaging sessions.

Because of selection rules, the 2P absorption properties of centrosymmetric dyes (such as D-A-D and A-D-A) may exhibit large wavelength shifts in their absorption spectra in solvents with varying polarity or under specific excitation conditions, with increases in cross-sectional values linked to the forbidden nature of the transitions at 2 x $\lambda_{max,\ 1PA}$ [19,32].

Here, the aim was to synthesise compounds with robust one-photon fluorescent properties and explore their two-photon possibilities. Much effort has been focused on donor–acceptor–donor (D-A-D) and donor–π–acceptor (D–π–A) derivatives with large 2PA cross sections, but they often struggle with dipole-induced aggregation and limited tunability of electronic transitions [33,34].

Thus we focused on the design, synthesise and evaluation of four new

* Corresponding author.
E-mail addresses: shufan.yang@ed.ac.uk (S. Yang), m.bradley@qmul.ac.uk (M. Bradley).

https://doi.org/10.1016/j.dyepig.2025.112785
Received 21 October 2024; Received in revised form 24 March 2025; Accepted 24 March 2025
Available online 24 March 2025

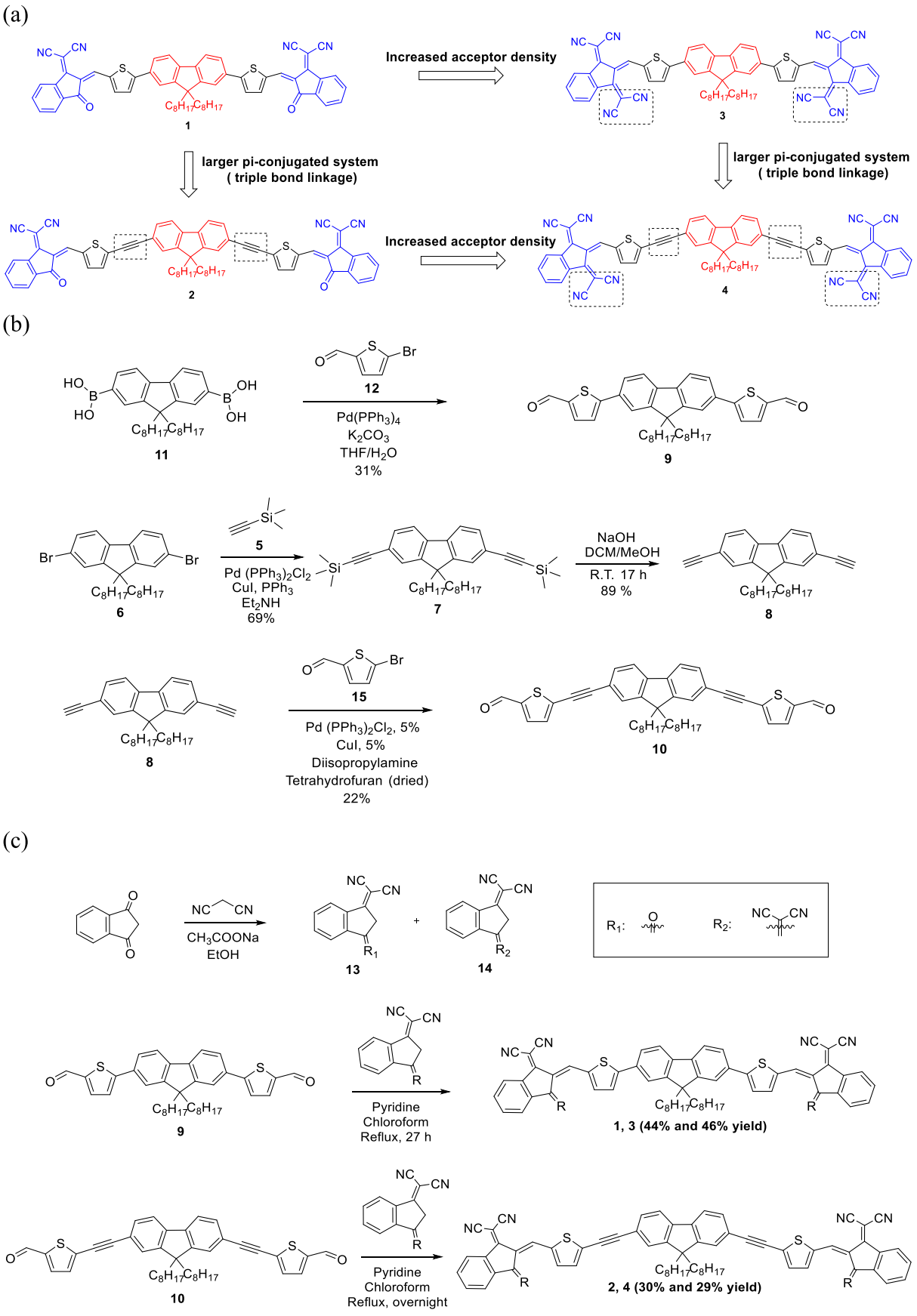

Fig. 1. (a): Synthetic strategy – increased conjugation and acceptor intensities of **1**–**4**. (b): Synthesis of the aldehydes **9** and **10**. (c): The condensation mediated synthesis of **1**–**4**.

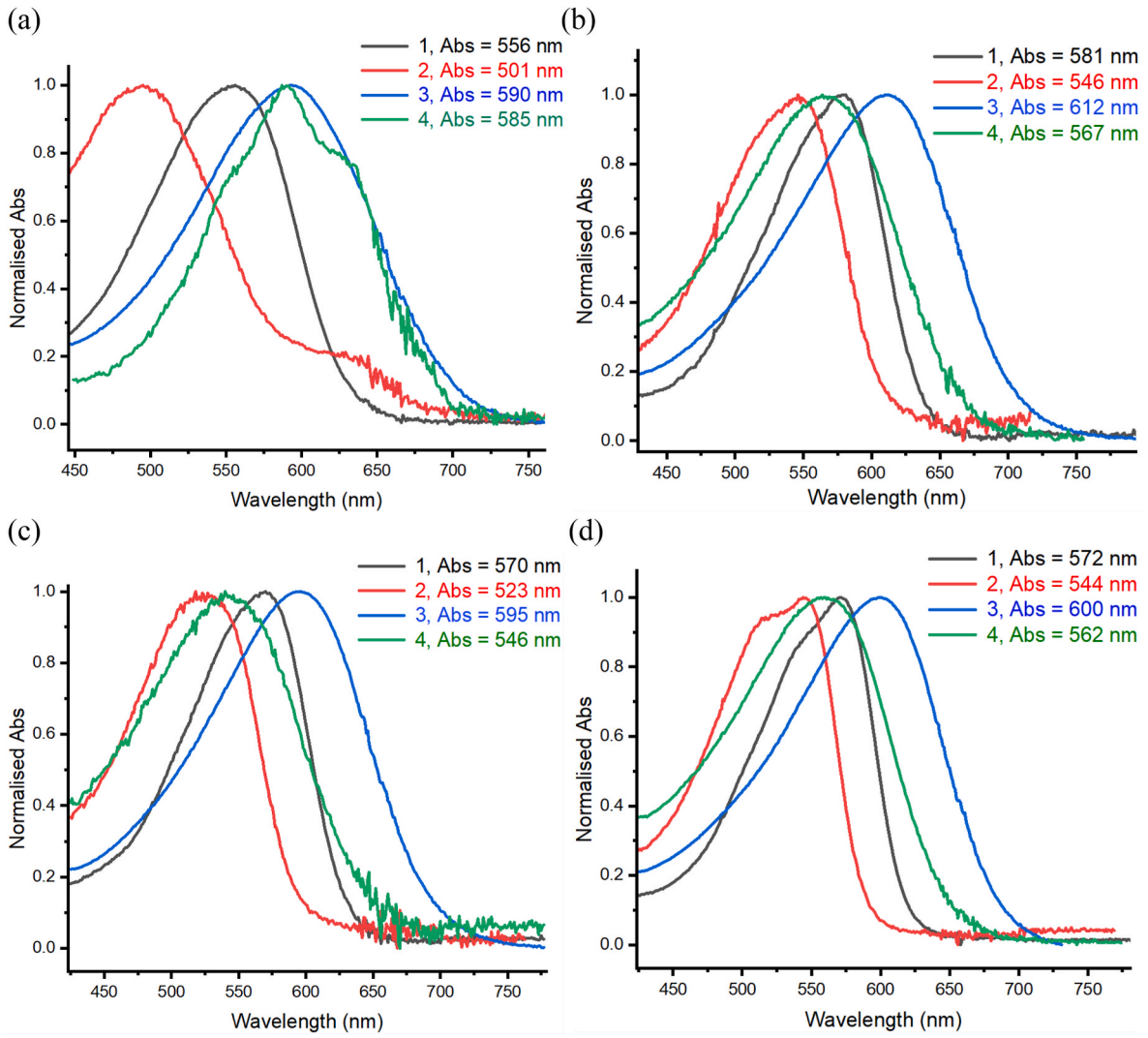

Fig. 2. Normalised UV–Vis analysis of **1**–**4** (5 μM) in: (a). Acetone (b). Dichloromethane; (c). Tetrahydrofuran; (d). Toluene. Data was collected from 450 to 750 nm.

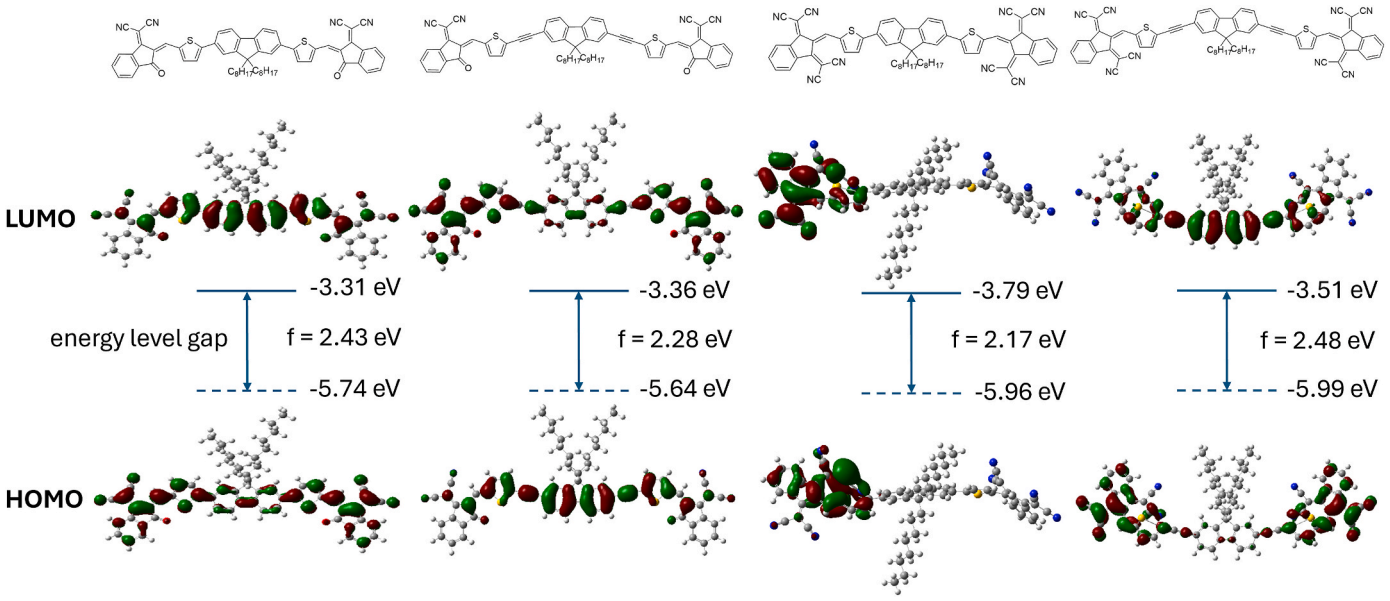

Fig. 3. Frontier molecular orbitals and energy levels (LUMO and HOMO) of **1**–**4** calculated using DFT at the B3LYP/6-31G* level using Gaussian 09 (see SI).

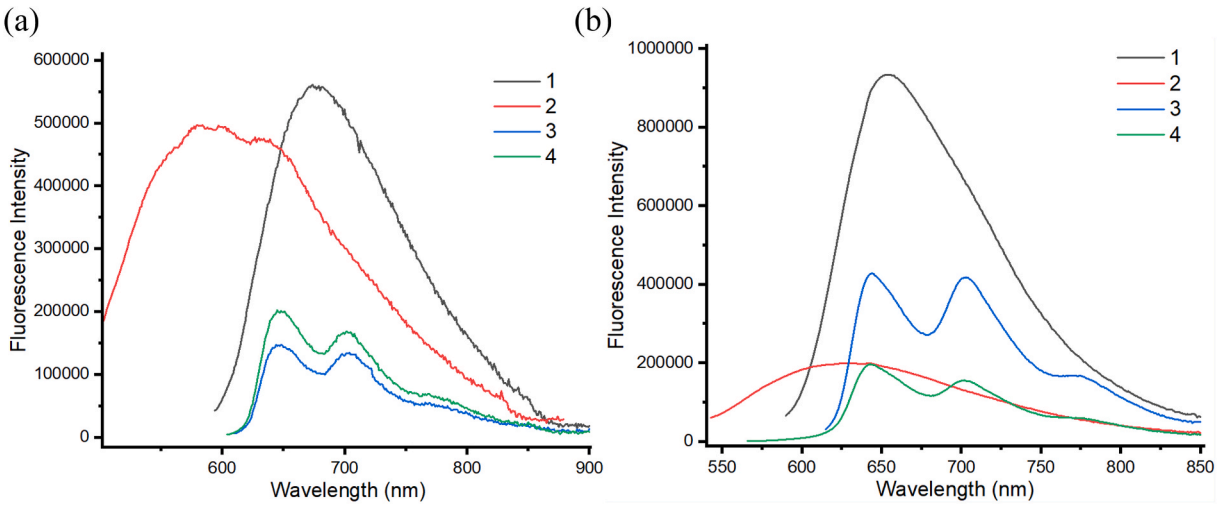

Fig. 4. (a): Fluorescence spectra of **1**–**4** in acetone (excited at each molecule's maximum λ_{abs}) and (b): In tetrahydrofuran. All at 5 μM. Bandwidth: 10 nm.

Table 1
The summary of 1P absorption, 1P fluorescence data and Stokes shifts of **1**–**4** in acetone and THF; Quantum yield measurements in acetone; 2P fluorescence data and 2P cross-section values in acetone; Extinction coefficients and 1P brightness in acetone.

Dye[a]	$\lambda_{abs,\ 1PA}$[b] nm	$\lambda_{abs,\ 1PA}$[c] (THF) nm	$\lambda_{em,\ 1PA}$[d] nm	$\lambda_{em,\ 1PA}$[e] (THF) nm	$\lambda_{em,\ 2PF}$[f] nm	$\delta_{max,\ 2PA}$[g] (GM)	Stokes shift[h] cm^{-1}	Stokes shift[i] (THF) cm^{-1}	Φ_F[j] %	ε[k] $cm^{-1}M^{-1}$	$\varepsilon \times \Phi_F$[l]
1	556	570	677	653	763	1716	3214	2230	0.7	180000	1260
2	501	523	618	627	692	782	3779	3172	0.4	70000	280
3	590	595	646	702	494	–	1470	2561	0.3	95000	285
4	585	546	700	703	491	–	2809	4091	0.04	97000	39

[a] The measurements of each of the dyes were carried out at 5 μM.
[b] UV–Vis measurements of **1**–**4** in acetone.
[c] UV–Vis measurements of **1**–**4** in THF.
[d] 1P fluorescence emission spectra of **1**–**4** in acetone (obtained by excitation at the maximum absorption wavelength of each dye).
[e] 1P fluorescence emission spectra of **1**–**4** in THF.
[f] 2P fluorescence measurements of **1**–**4.1** and **2** were excited at 1031 nm using a ps laser; **3** and **4** were excited using an 800 nm fs laser.
[g] 2PA cross-section values were obtained using a ps laser (λ = 1031 nm) for excitation in acetone (10^{-4} M), Rhodamine 6G was used as a reference [52–54].
[h] Stokes shift of **1**–**4** in acetone.
[i] Stokes shift of **1**–**4** in THF.
[j] The fluorescence quantum yields were determined relative to Rhodamine 6G in EtOH (ΦF = 0.94) [55] with each of the dyes at a concentration of 5 μM in acetone.
[k] Extinction coefficients (ε).
[l] One-photon brightness = extinction coefficient (ε) × one-photon fluorescence quantum yield (Φ_F).

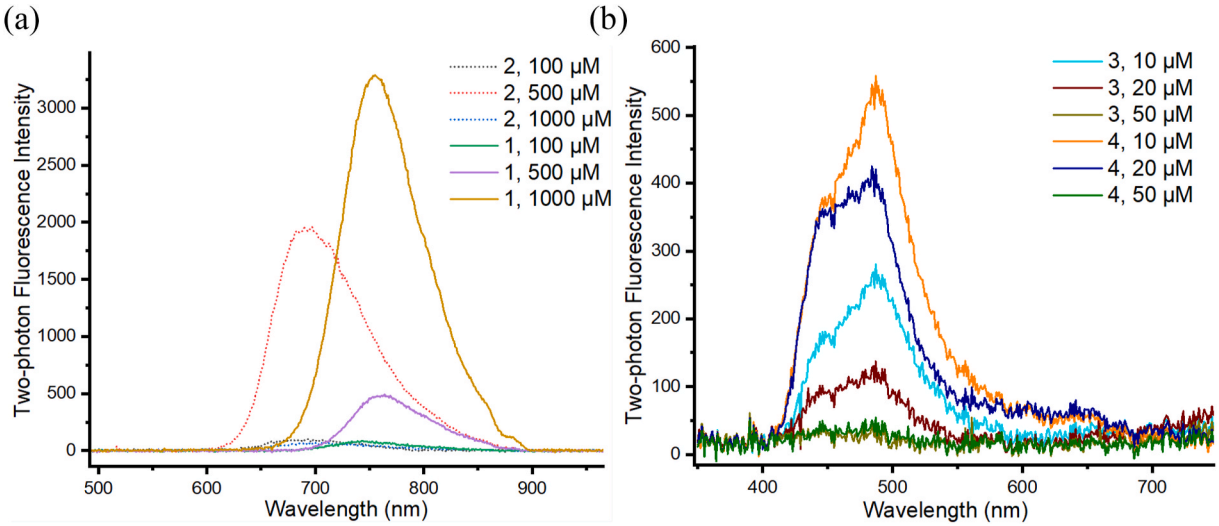

Fig. 5. (a): 2P fluorescence emission spectra of **1** and **2** at 100, 500 and 1000 μM in acetone (excited with a 1031 nm ps laser), 1 s exposure time. (b) Weak 2P fluorescence emission spectra of **3** and **4** at 10, 20 and 50 μM (using an 800 nm fs laser), 10 s exposure time.

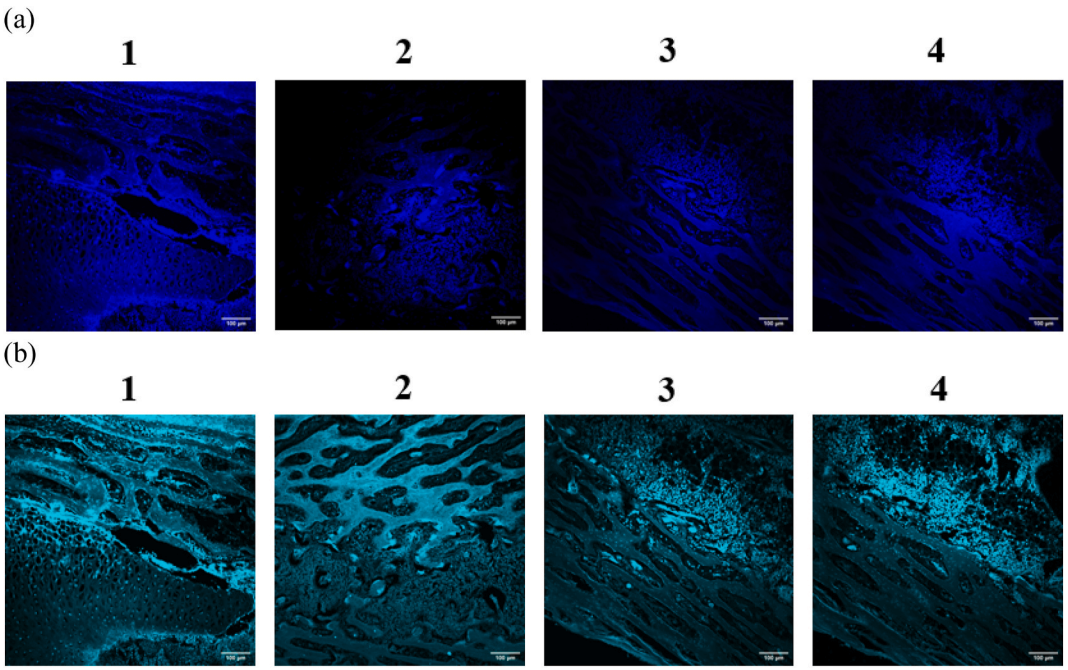

Fig. 6. Imaging of 18-day chick bone middle sections. (a): 1P imaging using fluorophores **1-4**, at 100 μM ((DMSO/Phosphate-buffered saline (1:9)) with an excitation wavelength of 405 nm (emission 419–685 nm). (b) 1P imaging of **1**–**4** at 100 μM with an excitation wavelength of 488 nm. All scale bars: 100 μm.

A-D-A dyes, exploring their 2PA properties and understanding the structure-property relationships across the structures. The A-D-A structure, especially when using fused-rings, tends to enhance their 2P absorbing efficiencies, attributed to the extended π-conjugation and strong intramolecular charge transfer (ICT) within the molecule [3,4,35–37]. Indeed, the integration of strong electron-donating and electron-withdrawing units in molecules facilitates charge redistribution, reducing the HOMO-LUMO energy gap and supporting efficient two-photon transitions [38–42]. Indeed, the ICT process can be fine-tuned through structural modifications, enhancing molecular polarizability and achieving higher 2PA cross-sections [43,44].

2. Result and discussion

Compounds **1–4** were synthesised, using fluorene as the donor core with two thiophenes as electron donating groups, attached either directly or via an alkyne bridge. 3-dicycanovinylindan-1-one and 1,3-bis (dicyanomethylidene)-indane were used as terminal acceptors due to their well-known (and powerful) electron-withdrawing properties/ strong electron-accepting capabilities which drives the charge transfer properties of the molecule - particularly beneficial for increasing the nonlinear optical properties such as 2 PA cross-sections [20,35].

It was expected that the triple bonds would increase the size of the pi-conjugated system across the molecules and provide red-shifted absorptions in 1PA and enhanced 2PA cross-sectional performance (Fig. 1a) [45]. Di-aldehyde **9** (Fig. 1b) was synthesised in one-step via a *bis*-Suzuki cross coupling between 5-bromothenaldehyde **15** and 9, 9-dioctylfluorene-2,7-diboronic acid **11** in 31 % yield. **10**, with its two triple bonds, was generated from 9,9-dioctyl-2,7-diethynefluorene **8** and Sonogashira coupling with 2 equivalents of 5-bromothenaldehyde **15**. **8** was itself synthesised from 9,9-dioctyl-2,7-dibromofluorene and trimethylsilyacetylene via a bis-Sonogashira coupling, with the silyl-groups of **7** removed using aqueous NaOH. 3-Dicycanovinylindan-1-one **13** and 1, 3-bis(dicyanomethylidene)-indane **14** were synthesised via condensation between 1,3-indandione and malononitrile, which were subsequently reacted with **9** and **10** to give the new fluorophores **1–4** (Fig. 1c).

The absorption and fluorescence spectra of **1**–**4** are shown in Fig. 2. The first observation was that they displayed quite remarkable variations in their optical properties depending on the solvent, a phenomenon known as solvatochromism [46–48]. Thus, **1** had a λ_{max} of 556 nm in acetone, but exhibited a 25 nm bathochromic shift (λ_{max} of 581 nm) in DCM and a 15 nm bathochromic shift in THF and toluene (all at 5 μM). Surprisingly the expected increase in conjugation in **2**, that would be anticipated to result in a bathochromic shift, showed the opposite effect in all solvents (λ_{max} was 501 nm in acetone, 546 nm in DCM, 523 nm in THF and 544 nm in toluene), suggesting that conjugation was actually reduced. **3**, which has strongest terminal acceptors, exhibited a bathochromic shift compared to **1** (34 nm in acetone (λ_{max} 590 nm), 31 nm in DCM (612 nm), 25 nm in THF (595 nm) and 28 nm in toluene (600 nm)) as expected. However, again, surprisingly, the alkyne system **4** showed a hypsochromic shift (compared to **3**) in these 4 solvents (λ_{max} 585 nm in acetone, 567 nm in DCM, 546 nm in THF and 562 nm in toluene). Thus, despite the expected increased pi-conjugation and strong terminal acceptor units strengthening the pull effect, the spectrum for **2** and **4** were not red-shifted. The rationale might be that conjugation with the alkyne and the fluorene (or the thiophene) leads to a relatively twisted orthogonal (rather than planer) orientation. In acetone, perhaps due to aggregation or some small population of extended conjugation, we see additional, but weak, lower energy bands at 650 nm for **2** and **4**. To better understand the structure-property relationship between **1**–**4**, the energy levels were calculated (see SI) and are shown in Fig. 3. The differences in HOMO-LUMO energy levels calculated for **1**–**3** were in close agreement to the observed energy level data obtained scopically, with a difference of less than 0.2 eV. Notably, **3** had the lowest energy gap in the calculations, which aligned with the experimental data.

The fluorescence spectra of **1**–**4** were collected (in acetone and THF), exciting each molecule at its maximum absorption (see Fig. 4). It was clear that all 4 molecules displayed large stokes shifts in acetone. **1** has a maximal emission at 677 nm, with a Stokes shift of 3214 cm^{-1} (121 nm), with **2** showing a similarly large Stokes shift (3779 cm^{-1} (117 nm), λ_{em} = 618 nm). **3** and **4** had emissions at 646 nm and 700 nm, exhibiting Stokes shifts of 1470 cm^{-1} and 2809 cm^{-1} respectively (110 nm and 115 nm), however, had much lower fluorescence intensities compared to **1** and **2**. Generally, the Stokes' shift and response to changes in polarity can be attributed to symmetry-breaking charge transfer, a known

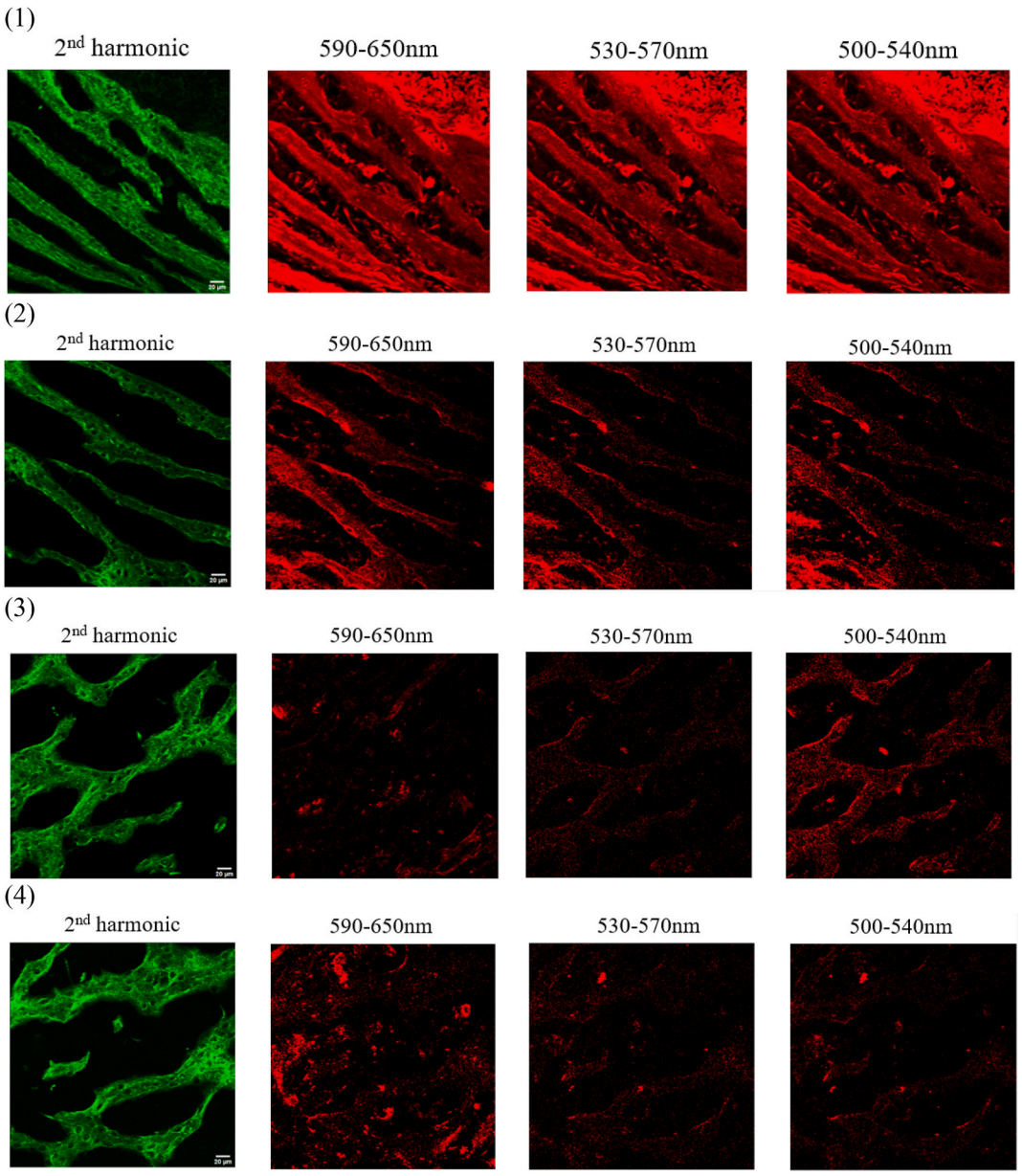

Fig. 7. Images (1-4) of 18-day chick bone middle sections of chick thigh bone stained with fluourophores **1**–**4 respectively**. Second-harmonic generation (SHG) (green) (400 nm) and two-photon fluorescence (TPF) images (red) with emission filters at 590–650 nm, 530–570 nm, and 500–540 nm. (excited with an 810 nm laser). Scale bar: 20 μm.

phenomenon in the excited state of quadrupolar dyes [49–51]. In THF, the molecules all showed similar properties as in acetone. Thus **1** had an $\lambda_{em(max)}$ at 653 nm with a Stokes shift of 2230 cm^{-1} (82 nm), while **2** had a Stokes shift of 3172 cm^{-1} (104 nm) (λ_{em} 627 nm). Expectedly, **3** and **4** showed lower fluorescence intensity (in THF, **3** had an λ_{em} 702 nm with a Stokes shift of 2561 cm^{-1} (177 nm) and **4** had a 4091 cm^{-1} (157 nm) Stokes shift (λ_{em} = 703 nm)). It was interesting to see that **3** and **4** showed almost the same fluorescence spectra whereas **1** and **2** exhibited major differences in emission and broadness of the emission.

Table 1 gives a summary of the 1P absorption and fluorescence data, Stokes shifts for compounds **1–4** in acetone and THF, quantum yield measurements, 2P fluorescence data and 2P cross-section values, as well as the extinction coefficients and 1P brightness. Fig. 5a shows the 2P fluorescence excitation of **1** and **2** at different concentrations. As the concentration increased, the 2P fluorescence increased up to 500 μM but then exhibited quenching. **3** and **4** exhibited essentially no 2P excited fluorescence even with higher laser powers under these conditions.

1P imaging was performed on 18-day chicken bones (middle section) stained with probes **1–4**, excited at 405 nm and 488 nm respectively. Fig. 6a demonstrates their dye staining ability, especially of **1** which offered good contrast under 405 nm excitation. Under 488 nm excitation, **1–4** exhibited good contrast with no significant differences among them (Fig. 6b). The bone samples were employed in second-harmonic imaging microscopy and two-photon fluorescence microscopy (looking at three emission wavelength ranges) to investigate the localisation and properties of the new dyes **1–4** (see Fig. 7), and showed good contrast of the tissue features. Specifically, **1** exhibited high brightness and good contrast, whereas **3** and **4** had the lowest brightness, but showed the best contrast at 500–540 nm.

3. Conclusions

We explored the design, synthesis and characterisation of 4 novel molecules based on an acceptor-donor-acceptor system exhibiting one-

photon and two-photon fluorescence properties. Notably, **1–4** exhibited high molar extinction coefficients (from 70000 $cm^{-1}M^{-1}$ to 180000 $cm^{-1}M^{-1}$) and exhibited large Stokes shift in one-photon studies (from 1470 cm^{-1} to 4090 cm^{-1}), presumably as a result of the centrosymmetric dyes having markedly different properties in the excited state. Surprisingly the expected pi-conjugation enhancement did not materialise, with the alkyne system of **4** showing a hypsochromic shift, perhaps due to twisting of the structure to negate full conjugation. DFT studies of the HOMOs and LUMOs showed energy gaps (2.43 eV, 2.28 eV, 2.17 eV and 2.48 eV) largely consistent with the optical properties of the fluorophores. **3** showed large, non-symmetrical, frontier molecular orbital density, perhaps a reflection of the four electron with-drawing nitrile end groups. **1** had a 2 PA cross-section value of $\delta = 1716$ GM, (**2** $\delta = 782$ GM), showcasing their potential for multiphoton applications. One-photon and two-photon imaging studies of the dyes **1–4** in day-18 chick bone were carried out and generated good contrast of bone morphology under both imaging modalities. Their bioimaging behaviour makes them promising tools for a range of single and multiphoton imaging applications, and future work will focus on further optimising these molecules and exploring their full potential in biomedical diagnostics.

CRediT authorship contribution statement

Shufan Yang: Writing – review & editing, Writing – original draft, Visualization, Validation, Software, Resources, Methodology, Investigation, Formal analysis, Data curation, Conceptualization. **Konstantinos Bourdakos:** Methodology, Investigation, Formal analysis. **Hiroki Cook:** Methodology, Investigation, Formal analysis, Data curation. **Anna Crisford:** Methodology, Formal analysis, Data curation. **Ewan Forsyth:** Supervision, Methodology, Formal analysis, Data curation. **Sumeet Mahajan:** Supervision, Methodology, Conceptualization. **Mark Bradley:** Writing – review & editing, Supervision, Project administration, Funding acquisition, Conceptualization.

Declaration of competing interest

There are no conflicts to declare.

Acknowledgements

We sincerely thank Dr. Maxime Klausen (Chimie ParisTech - PSL University, CNRS) for his invaluable guidance in refining this manuscript. We acknowledge the funding from the Engineering and Physical Sciences Research Council (EPSRC, United Kingdom) (grant EP/T020997).

Appendix A. Supplementary data

Supplementary data to this article can be found online at https://doi.org/10.1016/j.dyepig.2025.112785.

Data availability

See supplementary data.

References

[1] Zampetti A, et al. Highly efficient solid-state near-infrared organic light-emitting diodes incorporating A-D-A dyes based on α,β-unsubstituted "BODIPY" moieties. Sci Rep 2017;7(1):1611.
[2] Zhao J, et al. Recent advances in high-performance organic solar cells enabled by acceptor–donor–acceptor–donor–acceptor (A–DA′D–A) type acceptors. Mater Chem Front 2020;4(12):3487–504.
[3] He Z, et al. An acceptor–donor–acceptor structured small molecule for effective NIR triggered dual phototherapy of cancer. Adv Funct Mater 2020;30(16):1910301.
[4] Gong P, et al. Design of A-D-A-type organic third-order nonlinear optical materials based on benzodithiophene: a DFT study. Nanomaterials 2022;12. https://doi.org/10.3390/nano12203700.
[5] Liu Z, et al. Recent development of efficient A-D-A type fused-ring electron acceptors for organic solar. Sol Energy 2018;174:171–88.
[6] Zhang M, Ma Y, Zheng Q. Asymmetric indenothienothiophene-based unfused core for A-D-A type nonfullerene acceptors. Dyes Pigments 2020;180:108495.
[7] Chaudhary S, et al. Novel thiazoline-phenothiazine based "push-pull" molecules as fluorescent probes for volatile acids detection. J Photochem Photobiol Chem 2020;397:112509.
[8] Schneider F, Lippert E. Elektronenspektren und Elektronenstruktur von 9,9'-Dianthryl. Ber Bunsen Ges Phys Chem 1968;72(9–10):1155–60.
[9] Ivanov AI. Symmetry breaking charge transfer in excited multibranched molecules and dimers: a unified standpoint. J Photochem Photobiol C Photochem Rev 2024;58:100651.
[10] Pawlicki M, Latos-Grażyński L. A dynamic library of porphyrinic true nanorings. Angew Chem Int Ed 2012;51(45):11205–7.
[11] Pawlicki M, et al. Two-photon absorption and the design of two-photon dyes. Angew Chem Int Ed 2009;48(18):3244–66.
[12] He GS, et al. Multiphoton absorbing materials: molecular designs, characterizations, and applications. Chem Rev 2008;108(4):1245–330.
[13] Wang Y, et al. Two-photon excited deep-red and near-infrared emissive organic co-crystals. Nat Commun 2020;11(1):4633.
[14] Nag A, Goswami D. Solvent effect on two-photon absorption and fluorescence of rhodamine dyes. J Photochem Photobiol Chem 2009;206(2):188–97.
[15] TrÄGÅRdh J, et al. Exploration of the two-photon excitation spectrum of fluorescent dyes at wavelengths below the range of the Ti:Sapphire laser. J Microsc 2015;259(3):210–8.
[16] Bestvater F, et al. Two-photon fluorescence absorption and emission spectra of dyes relevant for cell imaging. J Microsc 2002;208(2):108–15.
[17] Guarin CA, et al. Two-photon absorption spectrum and characterization of the upper electronic states of the dye IR780. Spectrochim Acta Mol Biomol Spectrosc 2021;249:119291.
[18] Shimada T, et al. Molecular design for stable near-infrared-II two-photon excitation-induced photoacoustic contrast agents based on donor-substituted BODIPYs. ACS App Opti Mater 2024;2(1):211–9.
[19] Shaw PA, et al. Two-photon absorption: an open door to the NIR-II biological window? Front Chem 2022;10.
[20] Pascal S, et al. Near-infrared dyes for two-photon absorption in the short-wavelength infrared: strategies towards optical power limiting. Chem Soc Rev 2021;50(11):6613–58.
[21] Takasaki K, Abbasi-Asl R, Waters J. Superficial bound of the depth limit of two-photon imaging in mouse brain. eneuro 2020;7(1). ENEURO.0255-19.2019.
[22] Friedrich DM. Two-photon molecular spectroscopy. J Chem Educ 1982;59(6):472.
[23] Maharjan PS, Bhattarai HK. Singlet oxygen, photodynamic therapy, and mechanisms of cancer cell death. J Oncol 2022;2022:7211485.
[24] Robbins E, et al. Prospects for more efficient multi-photon absorption photosensitizers exhibiting both reactive oxygen species generation and luminescence. Molecules 2021;26(20):6323.
[25] Moreshead WV, et al. Design of a new optical material with broad spectrum linear and two-photon absorption and solvatochromism. J Phys Chem C 2013;117(44):23133–47.
[26] Li W, et al. Near-infrared absorbing porphyrin dyes with perpendicularly extended π-conjugation for dye-sensitized solar cells. RSC Adv 2014;4(92):50897–905.
[27] Shukla VK, et al. Red and NIR emitting ring-fused BODIPY/aza-BODIPY dyes. Dyes Pigments 2023;215:111245.
[28] Mütze J, et al. Excitation spectra and brightness optimization of two-photon excited probes. Biophys J 2012;102(4):934–44.
[29] Ośmiałowski B, et al. Controlling two-photon action cross section by changing a single heteroatom position in fluorescent dyes. J Phys Chem Lett 2020;11(15):5920–5.
[30] Luu P, Fraser SE, Schneider F. More than double the fun with two-photon excitation microscopy. Commun Biol 2024;7(1):364.
[31] Albota M, et al. Design of organic molecules with large two-photon absorption cross sections. Science 1998;281(5383):1653–6.
[32] Dore TM, Wilson HC. Chromophores for the delivery of bioactive molecules with two-photon excitation. In: Chambers JJ, Kramer RH, editors. Photosensitive molecules for controlling biological function. Totowa, NJ: Humana Press; 2011. p. 57–92.
[33] Sanyal S, et al. Aggregates of quadrupolar dyes for two-photon absorption: the role of intermolecular interactions. Phys Chem Chem Phys 2016;18(40):28198–208.
[34] Malval J-P, et al. Two-photon absorption in a conformationally twisted D–π–A oligomer: a synergic photosensitizing approach for multiphoton lithography. J Mater Chem C 2014;2(37):7869–80.
[35] Allen TG, et al. Highly conjugated, fused-ring, quadrupolar organic chromophores with large two-photon absorption cross-sections in the near-infrared. J Phys Chem 2020;124(22):4367–78.
[36] Chen Z, et al. Enhanced two-photon-excited fluorescence from electron donor-acceptor exciplex. Dyes Pigments 2021;188:109249.
[37] Susumu K, et al. Two-photon absorption properties of proquinoidal D-A-D and A-D-A quadrupolar chromophores. J Phys Chem 2011;115(22):5525–39.
[38] Genin E, et al. Fluorescence and two-photon absorption of push–pull aryl(bi)thiophenes: structure–property relationships. Photochem Photobiol Sci 2012;11(11):1756–66.

[39] Cai Z, et al. Two photon absorption study of low-bandgap, fully conjugated perylene diimide-thienoacene-perylene diimide ladder-type molecules. Chem Mater 2017;29(16):6726–32.
[40] Bureš F. Fundamental aspects of property tuning in push–pull molecules. RSC Adv 2014;4(102):58826–51.
[41] Wang J, et al. Self-assembled monolayers of push–pull chromophores as active layers and their applications. Molecules 2024;29. https://doi.org/10.3390/molecules29030559.
[42] Jiang H, et al. Tuning of the degree of charge transfer and the electronic properties in organic binary compounds by crystal engineering: a perspective. J Mater Chem C 2018;6(8):1884–902.
[43] Rout Y, et al. Multiple intramolecular charge transfers in multimodular donor–acceptor chromophores with large two-photon absorption. J Phys Chem C 2020;124(45):24631–43.
[44] Zhu S, Sun M. Photoinduced charge transfer in two-photon absorption. Res Opt 2021;4:100099.
[45] Tarsang R, et al. Triple bond-modified anthracene sensitizers for dye-sensitized solar cells: a computational study. RSC Adv 2015;5(48):38130–40.
[46] Homocianu M. Exploring solvatochromism: a comprehensive analysis of research data. Microchem J 2024;198:110166.
[47] Rauf MA, Hisaindee S. Studies on solvatochromic behavior of dyes using spectral techniques. J Mol Struct 2013;1042:45–56.
[48] Jabbar A, et al. A series of new acid dyes; study of solvatochromism, spectroscopy and their application on wool fabric. J Mol Struct 2019;1195:161–7.
[49] Verma P, et al. Excited-state symmetry breaking in quadrupolar pull–push–pull molecules: dicyanovinyl vs. cyanophenyl acceptors. Phys Chem Chem Phys 2023;25(34):22689–99.
[50] Dereka B, et al. Symmetry-breaking charge transfer and hydrogen bonding: toward asymmetrical photochemistry. Angew Chem Int Ed 2016;55(50):15624–8.
[51] Ivanov AI, Dereka B, Vauthey E. A simple model of solvent-induced symmetry-breaking charge transfer in excited quadrupolar molecules. J Chem Phys 2017;146(16):164306.
[52] Bradley DJ, et al. Interactions of picosecond laser pulses with organic molecules I. Two-photon fluorescence quenching and singlet states excitation in Rhodamine dyes. Proceedings of the Royal Society of London. A. Mathematical and Physical Sciences 1997;328(1572):97–121.
[53] Mongin O, et al. Synthesis, fluorescence, and two-photon absorption of a series of elongated rodlike and banana-shaped quadrupolar fluorophores: a comprehensive study of structure–property relationships. Chem Eur J 2007;13(5):1481–98.
[54] Xu C, Webb WW. Measurement of two-photon excitation cross sections of molecular fluorophores with data from 690 to 1050 nm. J Opt Soc Am B 1996;13(3):481–91.
[55] Fischer M, Georges J. Fluorescence quantum yield of rhodamine 6G in ethanol as a function of concentration using thermal lens spectrometry. Chem Phys Lett 1996;260(1):115–8.